

Impact of Cross-Diffusion on Methanol-Based Fe_3O_4 Nanofluid

Samrat Shivappa Payad ¹, Naramgari Sandeep ^{1,*}, Ram Prakash Sharma ²

¹ Department of Mathematics, Central University of Karnataka, Kalaburagi-585367, India

² Department of Mechanical engineering, National Institute of Technology Arunachal Pradesh, Yupia, Papum Pare District, Arunachal Pradesh, India

* Correspondence: nsandeep@cuk.ac.in;

Scopus Author ID 56626558400

Received: 10.11.2020; Revised: 5.12.2020; Accepted: 9.12.2020; Published: 12.12.2020

Abstract: This paper reports the impact of cross-diffusion on persistently moving a thin needle in a radiative hydromagnetic nanofluid flow. To validate the deviation in a border layer, we measured the flow features of two fluids such as methanol-magnetite and methanol. The converted ODEs are explicated by R-K centered shooting scheme. The consequences of extreme parameters on the existing profiles are depicted via graphs and numerical outcomes of tables. The study experiences that the velocity and temperature functions decrease with enhancing the needle size. The hypothesis of Soret and Dufour subjective to improve the thermal field, but it reduces the concentration. Further, it is noticed that the flow deterioration and strengthening of the thermal field have been perceived by the powers of Lorentz properties. The methanol-magnetite based nanofluid has higher thermal conductivity associated with methanol.

Keywords: MHD; thin needle; nanofluid; Soret-Dufour effect.

© 2020 by the authors. This article is an open-access article distributed under the terms and conditions of the Creative Commons Attribution (CC BY) license (<https://creativecommons.org/licenses/by/4.0/>).

1. Introduction

The boundary layer study over constantly moving objects has widespread features in fluid dynamics. In general, the flow characteristic depends on the object's fluid, speed, and shape characteristics. The present study initiates the boundary layer nature, the transmission of heat and mass over a constantly floating thin needle dipped in a nanofluid. There are various modifications and advances on the part of boundary layer nature. Many advanced techniques are utilized to augment flow properties by scientists and researchers. Lee [1] first recognized the nature of the boundary layer flow on the upper portion of a thin needle and subsequently studied the radial fluid motion solutions. Later, mixed convection flow on the thin needle surface is considered by Narain and Uberoi [2]. The characteristic of boundary layer flows carried around by the eventual surface of convection transport in free stream direction. This kind of flow largely occurs in the existence of moving cylindrical geometry reported by some investigators [3-5]. Heat transfer on an external surface of a thin needle under shrinking and stretching case by utilizing the Keller-box method was notified by Ahmed *et al.* [6]. An external flow of an incessantly wavering thin needle assumed parallel to axial flow was studied by Ishak *et al.* [7]. Abegurian *et al.* [8] discovered Casson's conduction possessions and Williamson liquid above a parallel plate. Chen and Kubler [9] considered a non-Newtonian liquid and heat transfer along floating tinny needles. The researchers [10-15] studied the heat transfer over the thin floating needle with various parameters and convective boundaries.

The problem of low conductivity reduces the performance of an industrial process. It is due to the use of low conductive fluids such as water, oil, methanol, etc. However, these sources are available in a large amount and are not negligible. Adding the conductive nano-sized solid particles in low conductive fluids enhance the thermal properties and known as nanofluids. Eastman *et al.* [16] justify that adding some conductive solid particles (0.5 Vol %) in water, methanol, and oil will highly enrich their thermal conductivity. Many authors acknowledged nanofluid properties that enrich and diminish the convection heat transfer. The present study reports the flow and heat transfer characteristics of Methanol-Fe₃O₄ nanoparticles. Siti *et al.* [17] analyzed the flow features of continually floating a needle deep in a nanoliquid. They noticed the influence of needle size and volume fraction to increase the heat flow rate. The heat flow behavior of nanoliquid over spherical tube was scrutinized by Sarkar *et al.* [18]. Sulochana *et al.* [19] examined the nanofluid and its conduction over an elongating sheet in the presence of radiation. Reddy *et al.* [20] reviewed the electromagnetic radiative nanoliquid above the parallel plate. They found that the magnetic field's influence decreases the flow velocity, but the thermal radiation increases the velocity. The nanoliquid behavior of thin-film and the non-Darcy medium were examined by Kumar *et al.* [21] and Sheikholeslami *et al.* [22].

The Dufour-Soret effects are ignored by many researchers in energy and the diffusion equation. Here, the bearing of Soret-Dufour constraints on MHD flow is unique for higher thermal and concentration gradients. It has plenteous usages in chemical engineering, solar collector, geophysical, environmental, etc. Boundary layer analysis and Soret-Dufour effects on an electromagnetic flow of nanofluid were studied by Reddy and Chamkha [23]. Free convection flow filled by nanofluid with Soret effect was investigated by Aly [24]. Babu and Sandeep [25] analyzed that the cross-diffusion influences the control of the species concentration and temperature function. Ramazan *et al.* [26] considered the eminence of Dufour and Soret properties in a viscoelastic liquid and evaluated by HAM. Zafar and Wiliam [27] inspected the Soret-Dufour impacts on linear convection transport over a vertical plate. Pal *et al.* [28] investigated MHD convection nanoliquid past wavering vertical plate with the existence of cross-diffusion and radiation properties. Reddy *et al.* [29] scrutinized the convective flow past a plate, cone, and wedge geometries under cross-diffusion and magnetic possessions by utilizing the R-K Fehlberg method. The radiation effect has substantial applications in industry and science. High-temperature processes, cancer treatments, space machinery, drilling process are some applications of radiation. Nasreen and Singh [30] presented the transport of coupled heat and mass due to a tinny needle's natural convection. They determined the radiation conflicts to magnify the temperature scatterings. Hayat *et al.* [31] and Sulochana *et al.* [32] simulated convective heat flow over the surface of a cylinder with thermal radiation. Ashraf *et al.* [33] and Khan *et al.* [34] studied the Soret/Dufour impacts and nanofluids' heat transport. Recently, the researchers [35-41] studied the impacts of the thermal radiation, Soret and Dufour parameters on various geometry and boundary conditions.

This study gives a numerical approach to the exterior flow of a constantly floating tinny needle saturated in radiative Methanol-Fe₃O₄ based nanofluid in the presence of Soret-Dufour effects. The systems of ODEs are resolved by adopting the R-K shooting technique. Computational results of heat, mass, and flow rates are tabulated and discussed. Increasing the needle thickness has the strength to reduce flow velocity. However, conflicting outcomes have been perceived for heat, mass flow rates of dual fluids. Precisely, the thermal and momentum aspects of methanol-magnetite nanoliquid decreased considerably as compared with methanol.

2. Methods

Consider a 2D-magnetohydrodynamic nanoliquid flow in the inactivity area of the moving thin needle. In Figure 1, let the coordinates of the cylinder be (x, r) , and an axial direction x -axis is normal to r , which is considered to be radial axis, and the needle thickness is labeled as c . We presumed the surface temperature of a cylinder is considerably superior to the ambient fluid. Correspondingly, $U_0 = u_w + u_\infty$ be the combined velocities along with the x -direction, where the needle velocity and conflicting normal velocity are respectively are u_w and u_∞ .

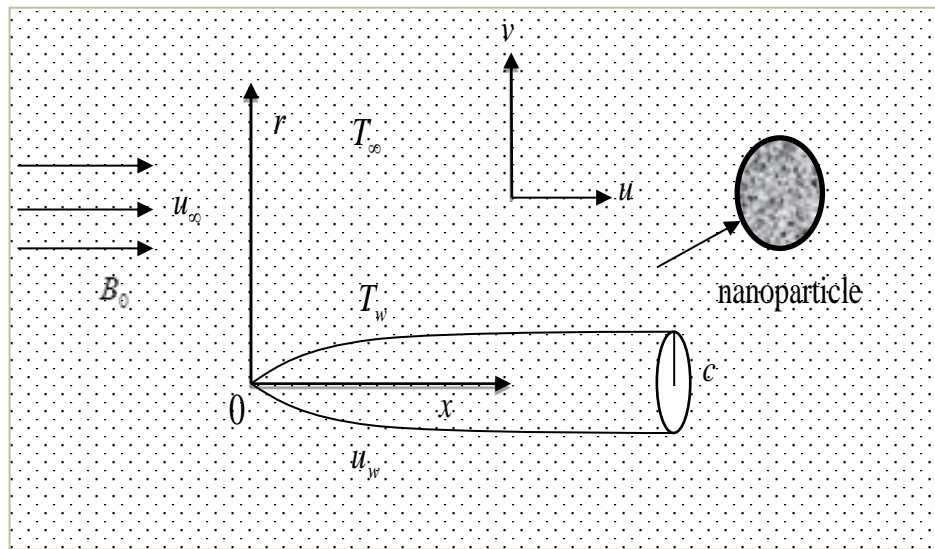


Figure 1. Geometry.

The electromagnetic field B_0 is enforced on the flow path direction and for infinitesimal magnitude of Reynolds number we neglected the induced magnetic properties. With reference to the above-considered conditions, the differential expressions are:

$$(ru)_x + (rv)_r = 0 \quad (1)$$

$$\rho_{nf} (uu_x + vv_r) = \mu_{nf} \frac{1}{r} (ru_r)_r - \sigma_{nf} B_0^2 u \quad (2)$$

$$(\rho C_p)_{nf} (uT_x + vT_r) = \frac{1}{r} \left[\left(\frac{16\sigma^* T_\infty^3}{3k^*} + k_{nf} \right) (rT_r)_r \right] + \frac{D_m K_T}{cs} \frac{1}{r} (rC_r)_r \quad (3)$$

$$uC_x + vC_r = \frac{D}{r} (rC_r)_r + \frac{D_m K_T}{T_m} \frac{1}{r} (rT_r)_r \quad (4)$$

The appropriate boundary limits are,

$$\begin{aligned} \text{at } r = R: C = C_w, u = u_w, T = T_w, v = 0, \\ u(\infty) \rightarrow u_\infty, C(\infty) \rightarrow C_\infty, T(\infty) \rightarrow T_\infty, \end{aligned} \quad (5)$$

where, u and v are velocity components to the radial and axial (x, r) directions. $k_{nf}, \mu_{nf}, (\rho C_p)_{nf}, \rho_{nf}$, are the thermal conductivity, viscosity, specific heat capacity, and density are specified as:

$$\begin{aligned} \rho_{nf} / \rho_f &= 1 - \phi \left(1 - \left(\rho_s / \rho_f \right) \right), \mu_f (1 - \phi)^{-2.5} = \mu_{nf}, \\ \left(\rho C_p \right)_{nf} / \left(\rho C_p \right)_f &= \left(1 - \phi \left(1 - \frac{\left(\rho C_p \right)_s}{\left(\rho C_p \right)_f} \right) \right), \sigma = \frac{\sigma_s}{\sigma_f}, \\ k_{nf} / k_f &= \frac{k_s + 2k_f - 2\phi k_f + 2\phi k_s}{2\phi k_f - 2\phi k_s + k_s + 2k_f}, \frac{\sigma_{nf}}{\sigma_f} = \frac{3\sigma\phi - 3\phi}{\sigma + 2 - \phi\sigma + \phi} + 1 \end{aligned} \quad (6)$$

We adopt the significant transformations as,

$$\psi = v_f x f(\eta), \eta = U_0 r^2 / v_f x, (T_w - T_\infty)(\theta(\eta)) = T - T_\infty, (C_w - C_\infty)(\varphi(\eta)) = C - C_\infty, \quad (7)$$

Here, ψ is identically resolved the continuity Eqn. (1) and the mechanisms well-defined as $u = \psi_r r^{-1}$, $v = -\psi_x r^{-1}$. Considering $\eta = c$, then Eqn. (7) calculates dimension of a needle $r = R(x) = \left(\frac{v_f c x}{U_0} \right)^{\frac{1}{2}}$ over the surface. By utilizing Eqn. (7) into Eqns. (2) to (5) produces ODEs,

$$2(1 - \phi)^{-2.5} (f'' + \eta f''') + \frac{\rho_{nf}}{\rho_f} f'' f' - M \frac{\sigma_{nf}}{\sigma_f} f' = 0, \quad (8)$$

$$\left((k_{nf} / k_f) + R \right) (\theta'' \eta + \theta') + \text{Pr} Du (\varphi'' \eta + \varphi') + \frac{\text{Pr}}{2} \left(\left(\rho C_p \right)_{nf} / \left(\rho C_p \right)_f \right) f \theta' = 0, \quad (9)$$

$$(\varphi'' \eta + \varphi') + \text{Sr} Sc (\theta'' \eta + \theta') + \frac{Sc}{2} f \varphi' = 0, \quad (10)$$

The appropriate boundary limits are,

$$\begin{aligned} f(c) &= (\lambda/2)c, f'(c) = (\lambda/2), \theta(c) = \varphi(c) = 1 \\ f'(\eta) &\rightarrow 1 - \lambda/2, \theta(\eta) \rightarrow (\lambda/2), \varphi(\eta) \rightarrow (\lambda/2) \text{ as } \eta \rightarrow \infty \end{aligned} \quad (11)$$

where, the velocity of needle is proportionate to the composite velocity directed as $\lambda = \frac{u_w}{U_0}$. In this report, $\lambda \leq 1$ is constrained to all specified boundaries. Therefore the free stream continuously carries in a favorable direction. The non-dimension factors $M, \text{Pr}, \text{Sr}, \text{Sc}, Du, R$, refers to the magnetic field, Prandtl number, Soret parameter, Schmidt number, Dufour and the radiation, respectively, constraint individually termed as,

$$\begin{aligned} \text{Sc} &= \frac{v_f}{D}, M = \frac{\sigma B_0^2}{2\rho U_0}, \text{Pr} = \frac{\mu C_p}{k_f}, R = \frac{16\sigma^* T_\infty^3}{3k^* k_f}, \\ \text{Sr} &= \frac{(T_w - T_\infty)}{(C_w - C_\infty)} \frac{D_m K_T}{T_m \mu C_p}, Du = \frac{(C_w - C_\infty)(D_m K_T)}{(cs \mu C_p)(T_w - T_\infty)}, \end{aligned} \quad (12)$$

The friction factor is,

$$\text{Re}_x^{1/2} C_f = \left(1 / (1 - \phi)^{2.5} \right) (4\sqrt{c}) f''(c), \quad (13)$$

The Nusselt number is,

$$(\text{Re}_x^{-1/2}) Nu_x = - \left(2\sqrt{c} \right) \left(k_{nf} / k_f + R \right) \theta'(c), \quad (14)$$

The Sherwood number is,

$$\text{Re}_x^{-1/2} Sh_x = -2D_B \sqrt{c} \varphi'(c), \quad (15)$$

where, $\text{Re}_x = (U_0 x / v_f)$.

3. Results and Discussion

The nonlinear Eqns. (8)-(10) accompanied by boundary precincts (11) are elucidated by effective R-K based shooting technique. This section discusses the heat and mass properties of $\text{Fe}_3\text{O}_4\text{-CH}_3\text{OH}$ based nanoliquid with the provision of tabular and graphical depiction for distinct dimensionless parameters on momentum, thermal and diffusion profiles, wall friction, transformed Sherwood and Nusselt factors. The non-dimensional quantities are considered as: $c = 0.1$, $\phi = 0.01$, $M = 1$, $\text{Pr} = 6$, $\lambda = 1$, $Du = Sr = 0.5$.

Table 1 directs the properties of CH_3OH and Fe_3O_4 molecules. The computational outcomes of physical constraints on the momentum, temperature function, and species fields have been reported in Tables 2 and 3. It was observed that the deviation of the dimensionless parameter does not show a substantial impact on the wall friction. As a result, methanol-magnetite nanofluid has greater conductive properties associated with methanol. The validation of the numerical approach is depicted in Table 4.

Figures 2 and 3 discuss the eccentricities of momentum and energy fields under extreme magnetic impacts, respectively. It was identified that increasing the magnetic arena's vitalities have shown the diminishing momentum profile and amplifies the thermal field. Indeed, the Lorentz force is augmented by increasing magnetic field. As a result, the flow deterioration and strengthening of the thermal field have been perceived by Lorentz properties' powers. The deviation of curves of the thermal field over the properties of radiation was established in Figure 4. As seen, larger values of thermal radiation amplify the temperature profile. Radiation produces external heat energy, which enriches the thermal field.

Figures 5 and 6 predict the Soret parameter's impact on the dimensionless thermal field and species concentration. It reflects that the benefits of the Soret parameter improve the thermal and weaken the concentration field. The Soret effect is a mixture of particles in fluids and depends on the density and concentration of a fluid. The Soret effect separates the mixed particles near the boundary layer and produces the buoyancy force, which increases the surface thickness, leads to augment temperature, and reduces the concentration field. Figures 7 and 8 elucidate the temperature and concentration fields for various Dufour parameters. Figure 7 noticed that the rise in Dufour parameter increases temperature field but the converse action, i.e., decreasing concentration field, is exposed in Figure 8.

The nature of velocity and thermal distribution for distinct needle thickness is exposed in Figures 9 and 10, respectively. It is renowned that escalating values of needle thickness denigrate both velocity and thermal field. The Schmidt number's thermal and concentration profiles for several bearings were elucidated in Figures 11 and 12.

Table 1. Thermo-physical properties.

Physical properties	Methanol	Fe_3O_4
$C_p (J/kgK)$	2545	670
$\rho (kg/m^3)$	792	5180
$K (w/mK)$	0.2035	9.7
$\sigma (s/m)$	0.5×10^{-6}	0.74×10^6

As seen in Figure 11, greater values of the Schmidt number augments the temperature profile. Simultaneously, the opposite trend has been seen in the concentration field, shown in Figure 12. Here, the Schmidt number is directly proportional to kinematic viscosity and

inversely proportional to Brownian diffusivity. Increasing Sc parameter creates an increasing trend in the thermal field. Also, it contributes to a lessening trend in the concentration field.

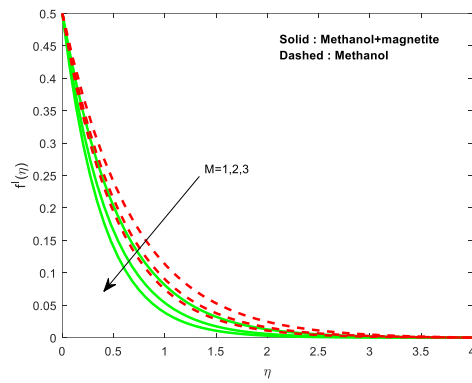


Figure 2. Impression of M on the flow field.

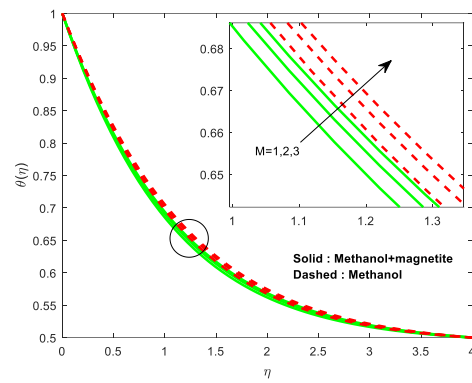


Figure 3. Impression of M on the thermal field.

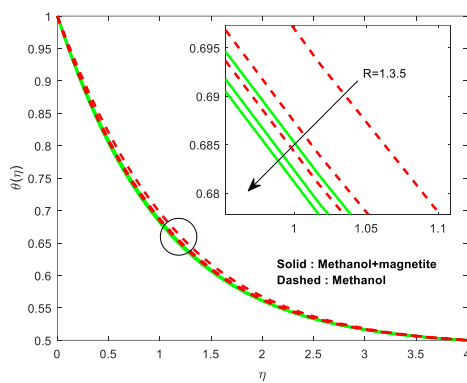


Figure 4. Impression of R on the thermal field.

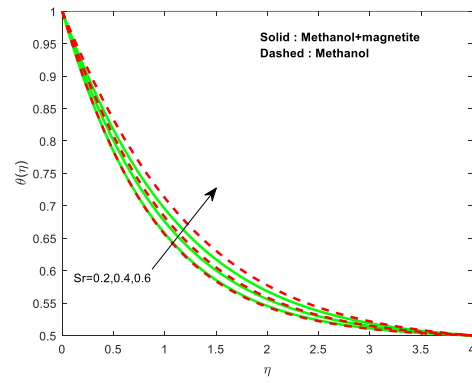


Figure 5. Impression of Sr on the thermal field.

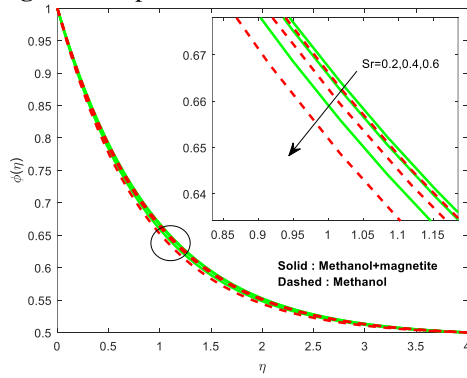


Figure 6. Impression of Sr on concentration field.

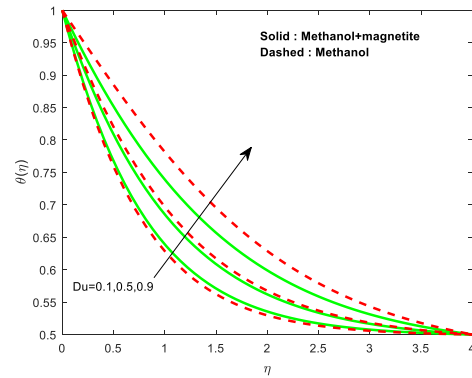


Figure 7. Impression of Du on the thermal field.

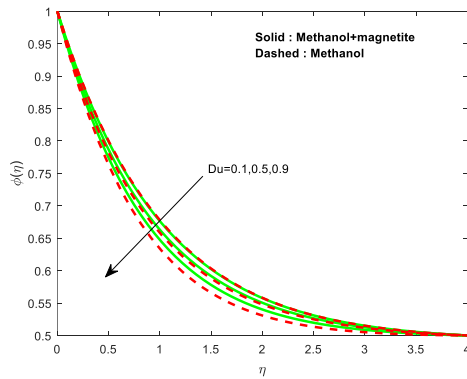


Figure 8. Impression of Du on concentration field.

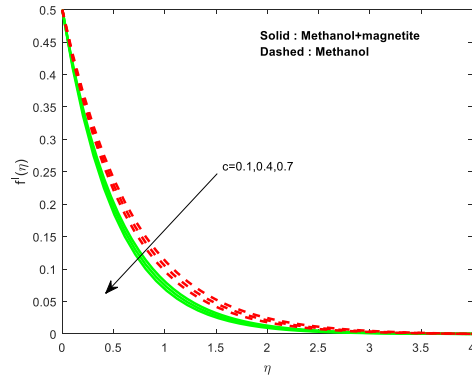


Figure 9. Impression of c on velocity field.

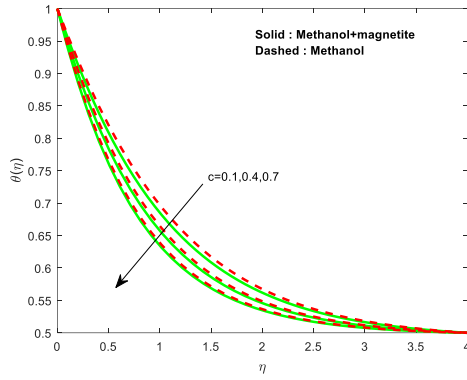


Figure 10. Impression of c on the thermal field.

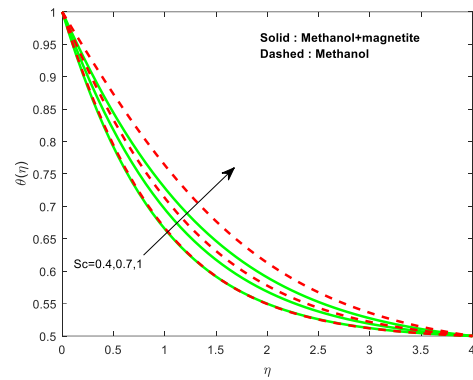


Figure 11. Impression of Sc on the thermal field.

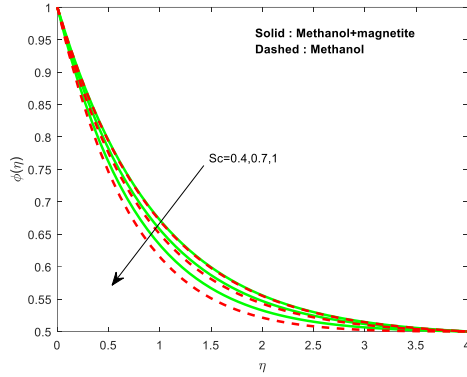


Figure 12. Impression of Sc on concentration field.

Table 2. Impression of physical parameters on C_f , Nu_x and Sh_x for Ethanol-magnetite nanofluid.

M	R	Sr	Du	c	Sc	C_f	Nu_x	Sh_x
1						-2.758816	0.638455	0.553852
2						-3.404377	0.625623	0.553813
3						-3.920416	0.617222	0.553813
	1					-2.758816	0.638455	0.553852
	3					-2.758816	0.664926	0.548138
	5					-2.758816	0.675734	0.545806
		0.2				-2.758816	0.754519	0.535686
		0.4				-2.758816	0.676709	0.544535
		0.6				-2.758816	0.600697	0.566340
			0.1			-2.758816	0.827939	0.513020
			0.5			-2.758816	0.638455	0.553852
			0.9			-2.758816	0.459044	0.592545
				0.1		-2.758816	0.638455	0.553852
				0.4		-6.438336	1.687436	0.556455
				0.7		-9.007709	2.624691	0.558293
					0.4	-2.758816	0.716321	0.527883
					0.7	-2.758816	0.600241	0.570777
					1.0	-2.758816	0.489013	0.636347

Table 3. Variation in C_f , Nu_x and Sh_x for Ethanol.

M	R	Sr	Du	c	Sc	C_f	Nu_x	Sh_x
1						-0.915718	0.266190	0.569372
2						-1.064014	0.261149	0.569727
3						-1.187920	0.257404	0.570017
	1					-0.915718	0.266190	0.569372
	3					-0.915718	0.294845	0.555950
	5					-0.915718	0.304089	0.551619
		0.2				-0.915718	0.343258	0.539233
		0.4				-0.915718	0.291396	0.554702
		0.6				-0.915718	0.241552	0.588439

M	R	Sr	Du	c	Sc	C_f	Nu_x	Sh_x
			0.1			-0.915718	0.394595	0.509344
			0.5			-0.915718	0.266190	0.569372
			0.9			-0.915718	0.149613	0.623906
				0.1		-0.915718	0.266190	0.569372
				0.4		-2.159051	0.725399	0.569610
				0.7		-3.049286	1.157014	0.568499
					0.4	-0.915718	0.318484	0.533163
					0.7	-0.915718	0.240874	0.592993
					1.0	-0.915718	0.168957	0.683522

Table 4. Validation of the numerical technique for Nu_x .

M	RKS (Present)	RKF	RKN
1	0.266190	0.2661904235	0.2661904234
2	0.261149	0.2611497654	0.2611497654
3	0.257404	0.2574043452	0.2574043453
4	0.243210	0.2432103125	0.2432103125

4. Conclusions

The study presents convective flow stability of $Fe_3O_4-CH_3OH$ based nanoliquid transport over a constantly floating tinny needle. Nonlinear differential equations are solved numerically by using the R-K shooting technique. We discussed MHD's influences, thermal radiation, chemical reaction, Soret and Dufour effects on velocity, thermal and concentration profile through graphs and friction factor, Nusselt number, and Sherwood number through tabular representation. The conclusions of the current study are as follows: An augmentation of thermal radiation R is caused by the Sherwood number's devaluation, but it increases the heat transfer rate. Also, radiation has the capacity to enlarge the thermal field; The dimensionless thermal field enriches due to bigger values of the Soret-Dufour parameter. Also, the concentration field diminishes by enlarging the Soret-Dufour parameter; Increasing the needle thickness has the strength to denigrate flow velocity, but it multiplies the Nusselt and Sherwood numbers; The border layer thickness accelerations for the benefits of Schmidt quantity. It observed the intensifying fields of thermal layer and Sherwood number; Nanofluids are widely consumed to raise or reduce the heat transfer; Methanol-magnetite-based nanofluid has higher thermal conductivity associated with methanol.

Funding

This research was funded by UGC-India, start-up grant number 30-489/2019(BSR).

Acknowledgments

This research was funded by UGC-India, start-up grant number 30-489/2019(BSR).

Conflicts of Interest

The authors declare no conflict of interest.

References

1. Lee, L.L. Boundary Layer over a Thin Needle. *The Physics of Fluids* **1967**, *10*, 820-822, <https://doi.org/10.1063/1.1762194>.
2. Narain, J.P.; Uberoi, M.S. Combined forced and free-convection over thin needles. *Int. J. Heat Mass Transfer* **1973**, *16*, 1505-1512, [https://doi.org/10.1016/0017-9310\(73\)90179-8](https://doi.org/10.1016/0017-9310(73)90179-8).
3. Narain, J.P.; Uberoi, M.S. Forced Heat Transfer over Thin Needles. *J. Heat Transfer* **1972**, *94*, 240-242, <https://doi.org/10.1115/1.3449910>.
4. Heo, J.-H.; Chung, B.-J. Natural convection heat transfer on the outer surface of inclined cylinders. *Chem. Eng. Sci.* **2012**, *73*, 366-372, <https://doi.org/10.1016/j.ces.2012.02.012>.
5. Takhar, H.S.; Chamkha, A.J.; Nath, G. Combined heat and mass transfer along a vertical moving cylinder with a free stream. *Heat Mass Transfer*. **2000**, *36*, 237-246, <https://doi.org/10.1007/s002310050391>.
6. Ahmad, S.; Arifin, N.M.; Nazar, R.; Pop, I. Mixed convection boundary layer flow along vertical thin needles: Assisting and opposing flows. *International Communications in Heat and Mass Transfer* **2008**, *35*, 157-162, <https://doi.org/10.1016/j.icheatmasstransfer.2007.07.005>.
7. Ishak, A.; Nazar, R.; Pop, I. Boundary Layer Flow over a Continuously Moving Thin Needle in a Parallel Free Stream. *Chinese Physics Letters* **2007**, *24*, 2895-2897, <https://doi.org/10.1088/0256-307X/24/10/051>.
8. Abegunrin, O.A.; Okhuevbie, S.O.; Animasaun, I.L. Comparison between the flow of two non-Newtonian fluids over an upper horizontal surface of paraboloid of revolution: Boundary layer analysis. *Alexandria Engineering Journal* **2016**, *55*, 1915-1929, <https://doi.org/10.1016/j.aej.2016.08.002>.
9. Chen, J.L.S.; Kubler, E.A. Non-Newtonian flow along needles. *The Physics of Fluids* **1978**, *21*, 749-751, <https://doi.org/10.1063/1.862293>.
10. Souayah, B.; Reddy, M.G.; Sreenivasulu, P.; Poornima, T.; Rahimi-Gorji, M.; Alarifi, I.M. Comparative analysis on non-linear radiative heat transfer on MHD Casson nanofluid past a thin needle. *J. Mol. Liq.* **2019**, *284*, 163-174, <https://doi.org/10.1016/j.molliq.2019.03.151>.
11. Sulochana, C.; Aparna, S.R.; Sandeep, N. Impact of linear/nonlinear radiation on incessantly moving thin needle in MHD quiescent Al-Cu/methanol hybrid nanofluid. *International Journal of Ambient Energy* **2020**, <https://doi.org/10.1080/01430750.2020.1768895>.
12. Waini, I.; Ishak, A.; Pop, I. Hybrid nanofluid flow past a permeable moving thin needle. *Mathematics* **2020**, *8*, 612, <https://doi.org/10.3390/math8040612>.
13. Tlili, I.; Nabwey, H.A.; Reddy, M.G.; Sandeep, N.; Pasupula, M. Effect of resistive heating on incessantly poignant thin needle in magnetohydrodynamic Sakiadis hybrid nanofluid. *Ain Shams Engineering Journal* **2020**, <https://doi.org/10.1016/j.asej.2020.09.009>.
14. Hashim; Hamid, A.; Khan, M. Thermo-physical characteristics during the flow and heat transfer analysis of GO-nanoparticles adjacent to a continuously moving thin needle. *Chinese Journal of Physics* **2020**, *64*, 227-240, <https://doi.org/10.1016/j.cjph.2019.12.003>.
15. Salleh, S.N.A.; Bachok, N.; Arifin, N.M.; Ali, F.M. Stability analysis of nanofluid flow past a moving thin needle subject to convective surface boundary conditions. *AIP Conf. Proc.* **2019**, *2184*, 060015, <https://doi.org/10.1063/1.5136447>.
16. Eastman, J.A.; Phillpot, S.R.; Choi, S.U.S.; Keblinski, P. Thermal Transport In Nanofluids. *Annual Review of Materials Research* **2004**, *34*, 219-246, <https://doi.org/10.1146/annurev.matsci.34.052803.090621>.
17. Soid, S.K.; Ishak, A.; Pop, I. Boundary layer flow past a continuously moving thin needle in a nanofluid. *Appl. Therm. Eng.* **2017**, *114*, 58-64, <https://doi.org/10.1016/j.applthermaleng.2016.11.165>.
18. Sarkar, S.; Ganguly, S.; Biswas, G.; Saha, P. Effect of cylinder rotation during mixed convective flow of nanofluids past a circular cylinder. *Computers & Fluids* **2016**, *127*, 47-64, <https://doi.org/10.1016/j.compfluid.2015.12.013>.
19. Samrat, S.P.; Sulochana, C.; Ashwinkumar, G.P. Impact of Thermal Radiation on an Unsteady Casson Nanofluid Flow Over a Stretching Surface. *International Journal of Applied and Computational Mathematics* **2019**, *5*, 31, <https://doi.org/10.1007/s40819-019-0606-2>.
20. Reddy, J.V.R.; Sugunamma, V.; Sandeep, N.; Sulochana, C. Influence of chemical reaction, radiation and rotation on MHD nanofluid flow past a permeable flat plate in porous medium. *Journal of the Nigerian Mathematical Society* **2016**, *35*, 48-65, <https://doi.org/10.1016/j.jnnms.2015.08.004>.
21. Anantha Kumar, K.; Sandeep, N.; Sugunamma, V.; Animasaun, I.L. Effect of irregular heat source/sink on the radiative thin film flow of MHD hybrid ferrofluid. *J. Therm. Anal. Calorim.* **2020**, *139*, 2145-2153, <https://doi.org/10.1007/s10973-019-08628-4>.
22. Sheikholeslami, M.; Keramati, H.; Shafee, A.; Li, Z.; Alawad, O.A.; Tlili, I. Nanofluid MHD forced convection heat transfer around the elliptic obstacle inside a permeable lid drive 3D enclosure considering lattice Boltzmann method. *Physica A: Statistical Mechanics and its Applications* **2019**, *523*, 87-104, <https://doi.org/10.1016/j.physa.2019.02.014>.
23. Reddy, P.S.; Chamkha, A.J. Soret and Dufour effects on MHD convective flow of Al₂O₃-water and TiO₂-water nanofluids past a stretching sheet in porous media with heat generation/absorption. *Adv. Powder Technol.* **2016**, *27*, 1207-1218, <https://doi.org/10.1016/j.appt.2016.04.005>.

24. Aly, A.M. Natural convection over circular cylinders in a porous enclosure filled with a nanofluid under thermo-diffusion effects. *Journal of the Taiwan Institute of Chemical Engineers* **2017**, *70*, 88-103, <https://doi.org/10.1016/j.jtice.2016.10.050>.
25. Babu, M.; Sandeep, D.N. MHD non-Newtonian fluid flow over a slendering stretching sheet in the presence of cross-diffusion effects. *Alexandria Engineering Journal* **2016**, *55*, <https://doi.org/10.1016/j.aej.2016.06.009>.
26. Ramzan, M.; Inam, S.; Shehzad, S.A. Three dimensional boundary layer flow of a viscoelastic nanofluid with Soret and Dufour effects. *Alexandria Engineering Journal* **2016**, *55*, 311-319, <https://doi.org/10.1016/j.aej.2015.09.012>.
27. Dursunkaya, Z.; Worek, W.M. Diffusion-thermo and thermal-diffusion effects in transient and steady natural convection from a vertical surface. *Int. J. Heat Mass Transfer* **1992**, *35*, 2060-2065, [https://doi.org/10.1016/0017-9310\(92\)90208-A](https://doi.org/10.1016/0017-9310(92)90208-A).
28. Pal, D.; Mandal, G.; Vajravalu, K. Soret and Dufour effects on MHD convective–radiative heat and mass transfer of nanofluids over a vertical non-linear stretching/shrinking sheet. *Applied Mathematics and Computation* **2016**, 287-288, 184-200, <https://doi.org/10.1016/j.amc.2016.04.037>.
29. Reddy, J.V.R.; Sugunamma, V.; Sandeep, N. Cross diffusion effects on MHD flow over three different geometries with Cattaneo-Christov heat flux. *J. Mol. Liq.* **2016**, *223*, 1234-1241, <https://doi.org/10.1016/j.molliq.2016.09.047>.
30. Singh, B.B. An integral treatment for heat and mass transfer along a vertical wall by natural convection in a porous media. *WIT Trans. Engng. Sci* **2007**, *56*, 143-151, <https://doi.org/10.2495/MPF070141>.
31. Hayat, T.; Tamoor, M.; Khan, M.I.; Alsaedi, A. Numerical simulation for nonlinear radiative flow by convective cylinder. *Results in Physics* **2016**, *6*, 1031-1035, <https://doi.org/10.1016/j.rinp.2016.11.026>.
32. Sulochana, C.; Samrat, S.P.; Sandeep, N. Boundary layer analysis of an incessant moving needle in MHD radiative nanofluid with joule heating. *International Journal of Mechanical Sciences* **2017**, 128-129, 326-331, <https://doi.org/10.1016/j.ijmecsci.2017.05.006>.
33. Bilal Ashraf, M.; Hayat, T.; Shehzad, S.A.; Ahmed, B. Thermophoresis and MHD mixed convection three-dimensional flow of viscoelastic fluid with Soret and Dufour effects. *Neural Computing and Applications* **2019**, *31*, 249-261, <https://doi.org/10.1007/s00521-017-2997-5>.
34. Ijaz Khan, M.; Hayat, T.; Afzal, S.; Imran Khan, M.; Alsaedi, A. Theoretical and numerical investigation of Carreau–Yasuda fluid flow subject to Soret and Dufour effects. *Comput. Methods Programs Biomed.* **2020**, *186*, 105145, <https://doi.org/10.1016/j.cmpb.2019.105145>.
35. Seyed, S.H.; Saray, B.N.; Chamkha, A.J. Heat and mass transfer investigation of MHD Eyring–Powell flow in a stretching channel with chemical reactions. *Physica A: Statistical Mechanics and its Applications* **2020**, *544*, 124109, <https://doi.org/10.1016/j.physa.2019.124109>.
36. Tlili, I.; Nabwey, H.A.; Samrat, S.P.; Sandeep, N. 3D MHD nonlinear radiative flow of CuO-MgO/methanol hybrid nanofluid beyond an irregular dimension surface with slip effect. *Sci. Rep.* **2020**, *10*, 9181, <https://doi.org/10.1038/s41598-020-66102-w>.
37. Salleh, S.N.A.; Bachok, N.; Arifin, N.M.; Ali, F.M. Influence of Soret and Dufour on forced convection flow towards a moving thin needle considering Buongiorno’s nanofluid model. *Alexandria Engineering Journal* **2020**, *59*, 3897-3906, <https://doi.org/10.1016/j.aej.2020.06.045>.
38. Tlili, I.; Samrat, S.P.; Sandeep, N.; Nabwey, H.A. Effect of nanoparticle shape on unsteady liquid film flow of MHD Oldroyd-B ferrofluid. *Ain Shams Engineering Journal* **2020**, <https://doi.org/10.1016/j.asej.2020.06.007>.
39. Kashyap, K.P.; Ojjela, O.; Das, S.K. Magnetohydrodynamic mixed convective flow of an upper convected Maxwell fluid through variably permeable dilating channel with Soret effect. *Pramana* **2019**, *92*, 73, <https://doi.org/10.1007/s12043-019-1732-4>.
40. Khan, S.A.; Hayat, T.; Ijaz Khan, M.; Alsaedi, A. Salient features of Dufour and Soret effect in radiative MHD flow of viscous fluid by a rotating cone with entropy generation. *Int. J. Hydrogen Energy* **2020**, *45*, 14552-14564, <https://doi.org/10.1016/j.ijhydene.2020.03.123>.
41. Bekezhanova, V.B.; Goncharova, O.N. Influence of the Dufour and Soret effects on the characteristics of evaporating liquid flows. *Int. J. Heat Mass Transfer* **2020**, *154*, 119696, <https://doi.org/10.1016/j.ijheatmasstransfer.2020.119696>.